Robust Functional Connectivity from MEG using Network Localized Granger Causality: Directional Connectivity Results in Physiological Frequency Bands

Behrad Soleimani*[1,2], Proloy Das[3], I.M. Dushyanthi Karunathilake[1,2], Joshua. P. Kulasingham[1,2], Stefanie E. Kuchinsky[4], Elisabeth B. Marsh[5], Jonathan Z. Simon[1,2,6], Behtash Babadi[1,2]

[1]Department of Electrical and Computer Engineering, University of Maryland, College Park, MD, [2]Institute for Systems Research, University of Maryland, College Park, MD, [3]Department of Anesthesia, Critical Care and Pain Medicine, Massachusetts General Hospital, Boston, MA, USA, [4]Audiology and Speech Pathology Center, Walter Reed National Military Medical Center, Bethesda, MD, USA, [5]Department of Neurology, the Johns Hopkins School of Medicine, Baltimore MD, USA, [6]Department of Biology, University of Maryland College Park, MD, USA

*behrad@umd.edu

Introduction

- Identifying causal relationships between different cortical areas for understanding mechanisms behind sensory processing
- Connectivity characterized by the temporal predictability of activity across brain regions via Granger causality (GC)
- Challenges with Magnetoencephalography (MEG): the data are low-dimensional, noisy, and linearly mixed versions of underlying source activities
- Conventional methods (two-stage procedure):

- Drawbacks: bias propagation, spatial leakage
- Goal: *directly* localize GC influences without an intermediate source localization step
- Method: Network Localized Granger Causality (NLGC)

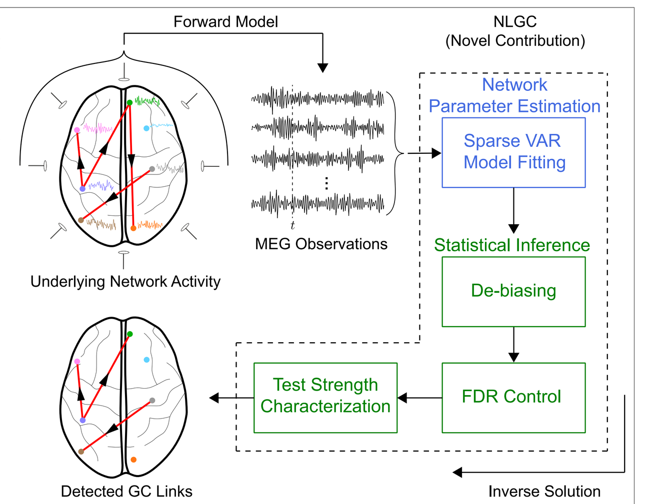

Fig. 1. Schematic depiction of the proposed NLGC inference. Without an intermediate source localization, the cortical connectivity is obtained directly from MEG observations.

Model

- Observation model:

$$\mathbf{y}_t = \mathbf{C}\mathbf{x}_t + \mathbf{n}_t, \quad t = 1, 2, \cdots, T$$

$\mathbf{y}_t \in \mathbb{R}^M$ MEG observation, $\mathbf{C} \in \mathbb{R}^{M\times N}$ lead field matrix
$\mathbf{x}_t \in \mathbb{R}^N$ source activity, $\mathbf{n}_t \in \mathbb{R}^M$ measurement noise

- Source dynamic model (auto-regressive):

$$\mathbf{x}_t = \sum_{k=1}^{q} \mathbf{A}_k \mathbf{x}_{t-k} + \mathbf{w}_t, \quad t = 1, 2, \cdots, T$$

$\mathbf{A}_k \in \mathbb{R}^{N\times N}$ coefficient matrix, $\mathbf{w}_t \in \mathbb{R}^N$ noise process

- Distributional assumptions:
  - $\mathbf{n}_t \sim$ zero-mean Gaussian (known covariance)
  - $\mathbf{w}_t \sim$ zero-mean Gaussian, independent sources (unknown diagonal covariance $\mathbf{Q}$)

Granger Causality

- Consider link $(\tilde{i} \to i)$ with following models:

$$\text{Full: } \mathbf{x}_t^{(i)} = \sum_j \sum_k a_{i,j,k} \mathbf{x}_{t-k}^{(j)} + \mathbf{w}_t^{(i)}, \quad \mathbf{w}_t^{(i)} \sim \mathcal{N}(0, \sigma_i^2)$$

$$\text{Reduced: } \mathbf{x}_t^{(i)} = \sum_{j\neq\tilde{i}} \sum_k a'_{i,j,k} \mathbf{x}_{t-k}^{(j)} + \mathbf{w'}_t^{(i)}, \quad \mathbf{w'}_t^{(i)} \sim \mathcal{N}(0, \sigma_{i\setminus\tilde{i}}^2)$$

- Granger Causality (GC) measure:

$$\mathcal{F}_{(\tilde{i}\to i)} = \log\left(\frac{\sigma_{i\setminus\tilde{i}}^2}{\sigma_i^2}\right)$$

relative predictive variance explained

- $\mathcal{F}_{(\tilde{i}\to i)} \gg 0$: GC link exists.

Fig. 2. GC link $(\tilde{i} \to i)$ implies temporal predictability of source i by $\tilde{i}$.

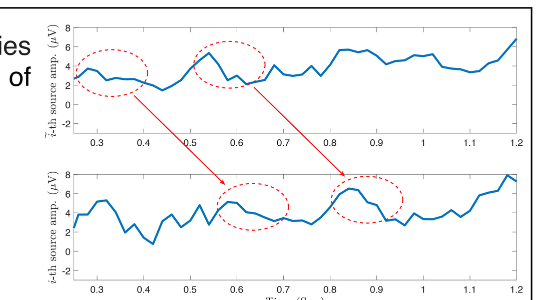

Parameter Estimation†

- Challenge: source activities are unknown
- Solution: Expectation Maximization (EM)
- At the l-th iteration:

$$\text{E-step}: \ Q(\boldsymbol{\theta}|\widehat{\boldsymbol{\theta}}^{(l)}) = \mathrm{E}\left[\log p(\mathbf{x}_{1:T}, \mathbf{y}_{1:T}; \boldsymbol{\theta}) \middle| \mathbf{y}_{1:T}; \widehat{\boldsymbol{\theta}}^{(l)}\right]$$

$$\text{M-step}: \ \widehat{\boldsymbol{\theta}}^{(l+1)} = \underset{\boldsymbol{\theta}}{\operatorname{argmax}} \left\{Q(\boldsymbol{\theta}|\widehat{\boldsymbol{\theta}}^{(l)}) + R_{\ell_1}(\boldsymbol{\lambda}, \boldsymbol{\theta})\right\}$$

- ℓ_1-norm regularization is utilized at the M-step to mitigate the ill-posedness resulting from the low-dimensional measurements

Statistical Inference†

- Two hypothesis for link $(\tilde{i} \to i)$:
  - $H_{(\tilde{i}\to i),0}$: there is no GC influence
  - $H_{(\tilde{i}\to i),1}$: there is a GC influence
- Asymptotic distributions:

$$[\mathcal{D}_{(\tilde{i}\to i)} | H_{(\tilde{i}\to i),0}] \xrightarrow{d} \chi^2(q)$$

$$[\mathcal{D}_{(\tilde{i}\to i)} | H_{(\tilde{i}\to i),1}] \xrightarrow{d} \chi^2(q, \nu_{(\tilde{i}\to i)})$$

- False discovery rate (FDR) control:
  - Reject null hypothesis at a confidence level α
  - Control FDR via BY procedure

†For details and more explanations, please check the paper.

Results: Synthetic Data†

Fig. 3. Comparison of NLGC with two-stage procedures using a realistic simulation setting. **A.** Example of the ground truth GC network, and estimates obtained by NLGC and two-stage approaches based on MNE, dSPM, and Champagne overlaid on dorsal and lateral brain plots. NLGC captures nearly all the existing GC links with no spurious detection. **B.** ROC curves (hit rate vs. false alarm) corresponding to NLGC, and two-stage approaches for exact/relaxed link localization and in the presence/absence of model mismatch. NLGC provides equal or better hit rate, while consistently maintaining low false alarm rate. **C.** Evaluating the effect of SNR in presence/absence of model mismatch. NLGC consistently maintains low false alarm rates across a wide range of SNR settings.

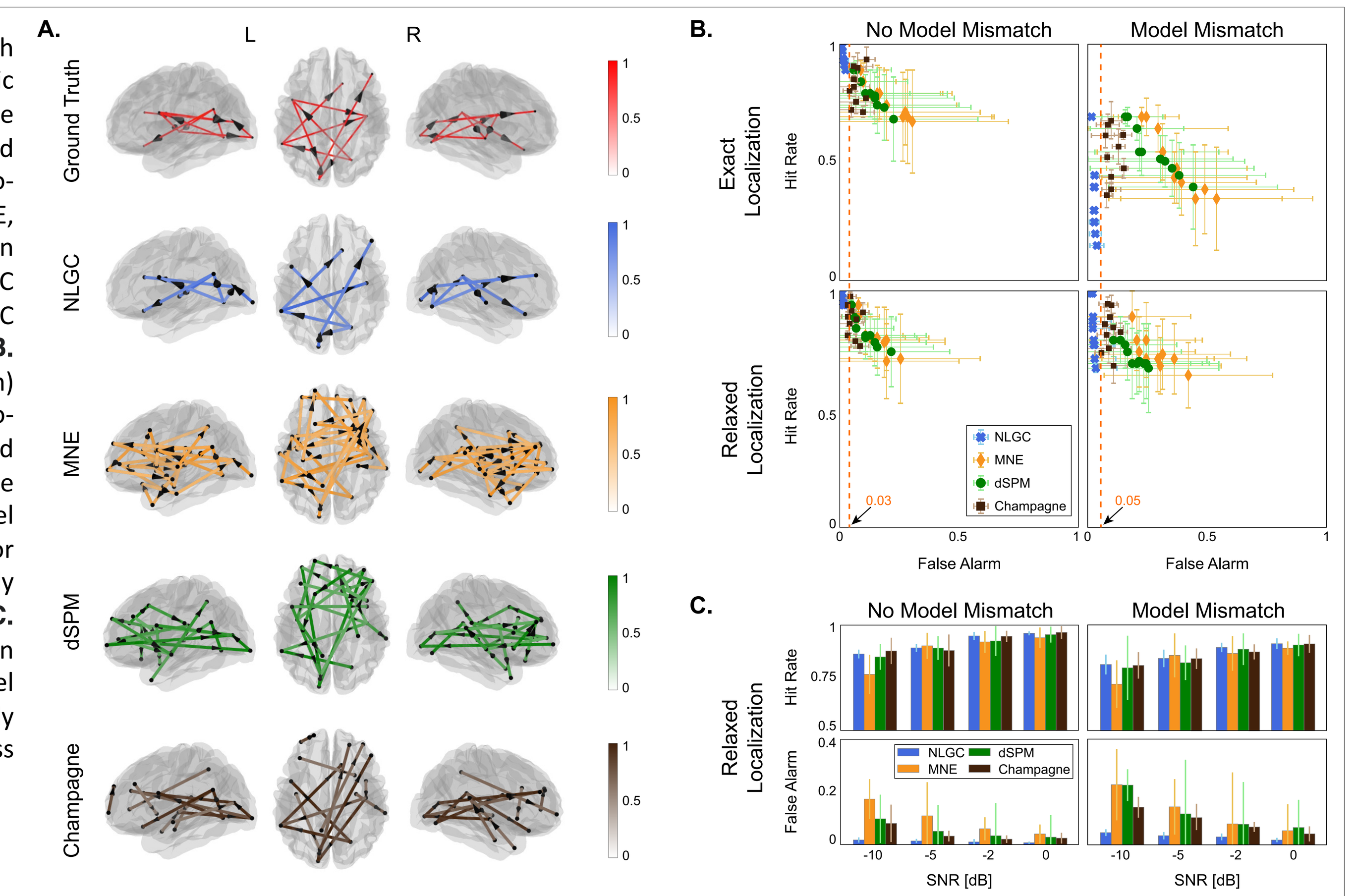

Results: Tone Processing vs. Resting State†

- 13 younger and 9 older adults
- 100 repetitions of tone pips presented at the end of resting state recordings
- Two 40 seconds trials per subject/condition
- Connectivity in auditory cortex is investigated

Fig. 4. NLGC analysis of experimentally recorded MEG data in two frequency bands. **A.** Extracted GC links between frontal and temporal areas overlaid on dorsal brain plots for younger (top row) and older (bottom row) participants in 0.1-8 Hz. There is a notable increase of top-down links from frontal to temporal areas during tone processing as compared to the resting state. **B.** Percentage of causal links, averaged over subjects within each age group, between frontal, temporal, and parietal areas for tone processing vs. resting state conditions and younger vs. older participants in 0.1-8 Hz. The dashed ovals indicate the normalized average number of links shown in panel A. There are notable changes across task conditions, including dominantly top-down frontal to temporal/parietal connections during tone processing, in contrast to dominantly bottom-up temporal/parietal to frontal connections during resting state. **C.** Extracted GC links between frontal and parietal areas overlaid on dorsal brain plots for younger (top row) and older (bottom row) participants in 13-25 Hz. There is a notable increase of frontal to parietal links under tone processing for older adults. **D.** Percentage of causal links, averaged over subjects within each age group, between frontal, temporal, and parietal areas for tone processing vs. resting state conditions and younger vs. older participants. The dashed ovals indicate the normalized average number of links shown in panel C. There are notable changes across both task conditions and age groups, including the higher involvement of parietal areas during resting state, increase of frontal to frontal connections for younger participants and top-down links from frontal to parietal areas for older participants, during tone processing.

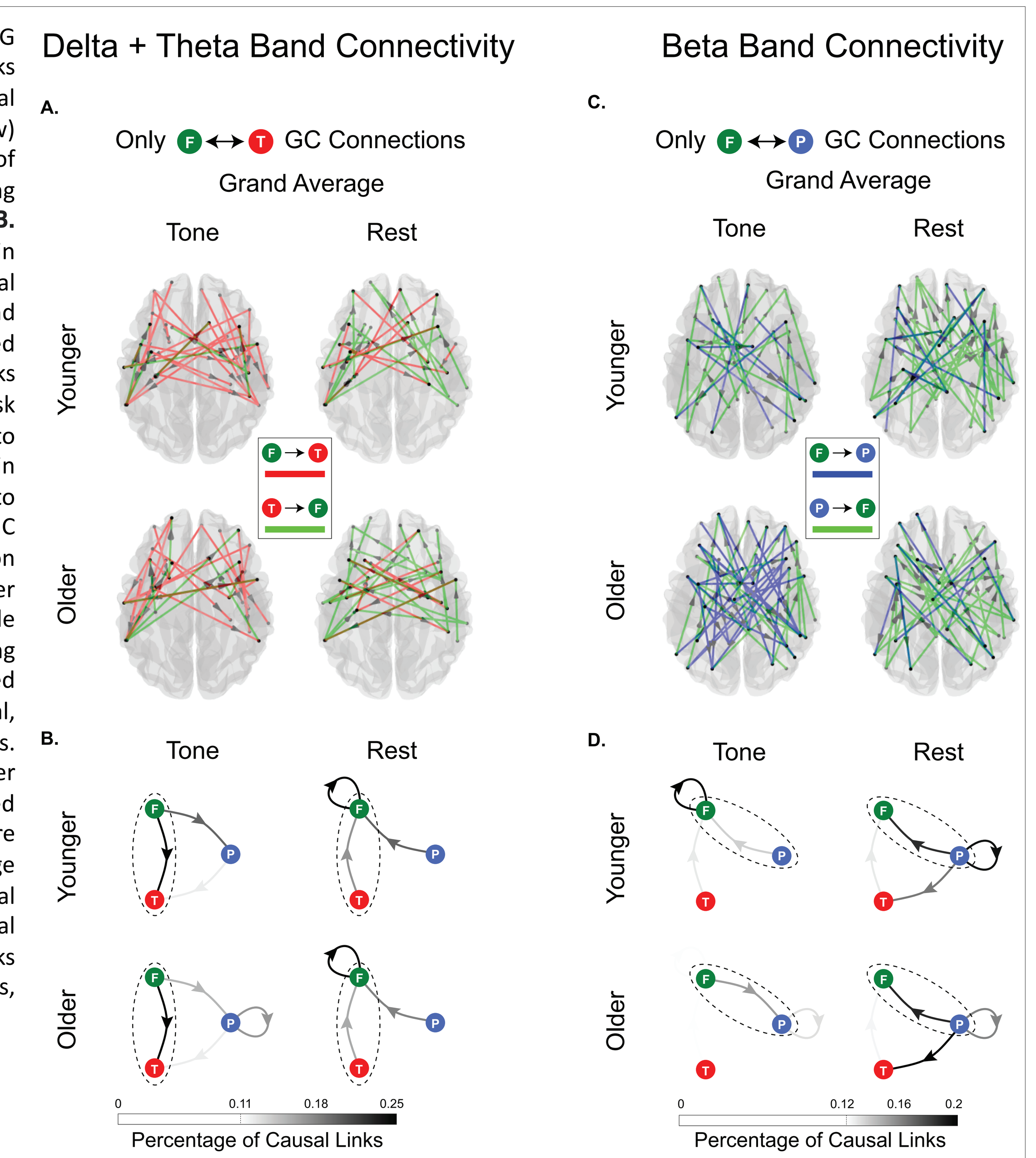

Results: Minor Stroke Patients

- 6 minor stroke patients undergoing clinical recovery and 6 controls
- 60 seconds resting state data recorded in two 6-month apart visits
- Frontoparietal (FPC) and non-FPC areas considered for connectivity analysis in beta band (13-25 Hz)
- Experimental details: Marsh, Elisabeth B., et al. "Poststroke acute dysexecutive syndrome, a disorder resulting from minor stroke due to disruption of network dynamics." Proceedings of the National Academy of Sciences 117.52 (2020): 33578-33585.

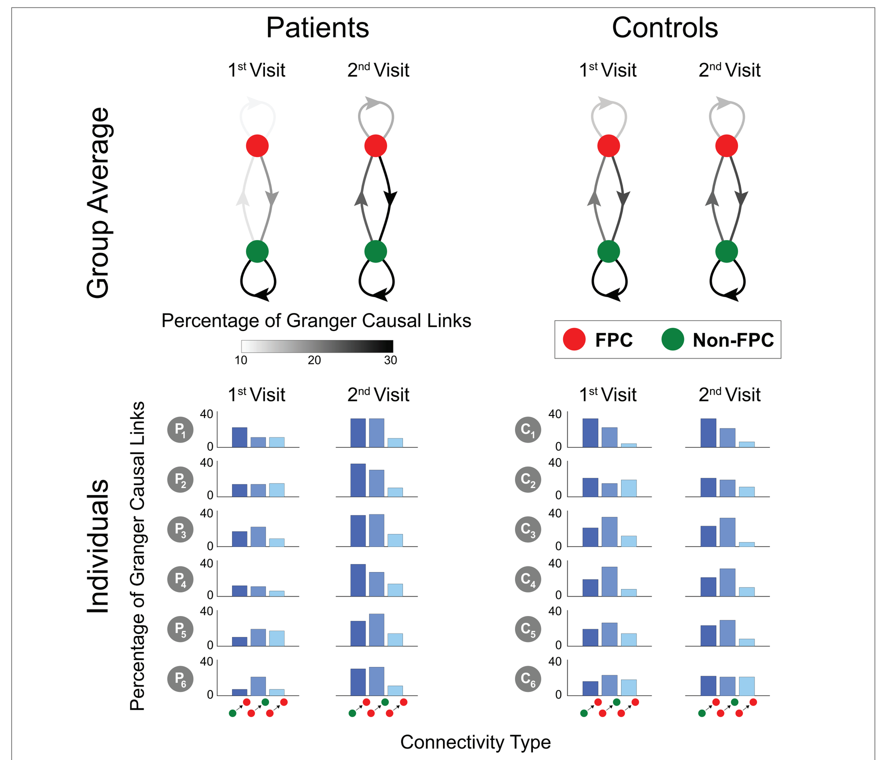

Fig. 5. FPC connectivity changes across visits for both patients and controls. The network does not change significantly across visits for controls. In contrast, for the patients FPC becomes more involved.

Results: Difficult Listening Experiment

- 1-minute-long speech segments from an audio book in two conditions:
  1) Clean speech (*easy*)
  2) Mixed speech: two talker speech, male vs. female speaker (*difficult*); task: attend to pre-specified speaker

Fig. 6. NLGC analysis of experimentally recorded MEG data in Theta band. **A.** Extracted GC links between frontal and temporal areas overlaid on dorsal brain plots for both age groups and conditions. There is a notable increase of top-down links from frontal to temporal areas of younger adults as listening becomes difficult but not the older participants. **B.** Percentage of causal links, averaged over subjects within each age group, between frontal, temporal, and parietal areas for easy and difficult conditions. There are notable changes across listening conditions as well as age. Frontal to temporal connections for older adults does not change significantly across listening conditions as opposed to younger adults.

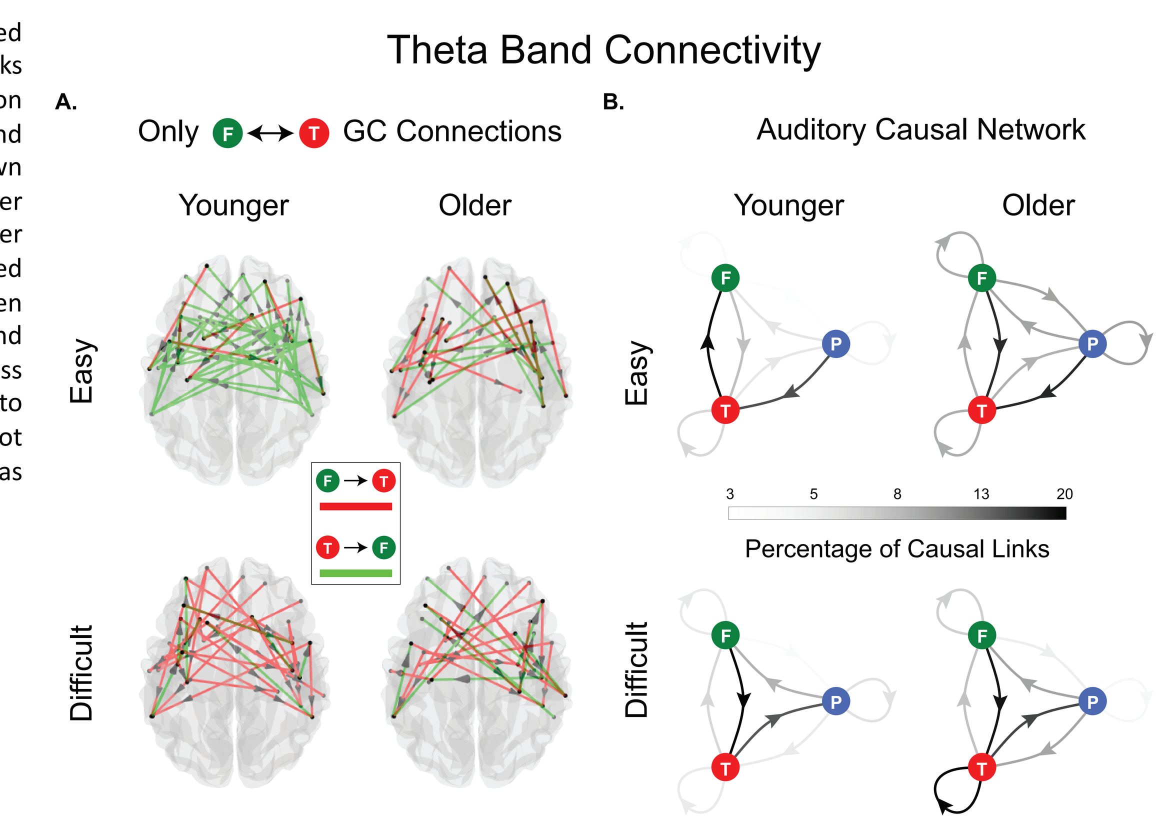

Reference

Paper:
Soleimani B, Das P, Karunathilake IMD, Kuchinsky SE, Simon JZ, Babadi B. NLGC: Network Localized Granger Causality with Application to MEG Directional Functional Connectivity Analysis. bioRxiv preprint (2022) DOI: https://doiorg/101101/2022030948368320222

Python Package:
Soleimani B, Das P. Network Localized Granger Causality. (2022) GitHub Repository at https://github.com/BabadiLab/NLGC

Supported by NSF (OISE2020624, SMA1734892 and CCF1552946) and NIH (R01-DC019394, R01- 970 DC014085, P01-AG055365, and R21-AG068802).